JMEPEG (2010) 19:185–193
DOI: 10.1007/s11665-009-9452-4

1059-9495/$19.00

Artificial Neural Networks for Surface Roughness Prediction when Face Milling Al 7075-T7351

Patricia Muñoz-Escalona and Paul G. Maropoulos

(Submitted October 9, 2008; in revised form March 2, 2009)

In this work, different artificial neural networks (ANN) are developed for the prediction of surface roughness (R_a) values in Al alloy 7075-T7351 after face milling machining process. The radial base (RBNN), feed forward (FFNN), and generalized regression (GRNN) networks were selected, and the data used for training these networks were derived from experiments conducted using a high-speed milling machine. The Taguchi design of experiment was applied to reduce the time and cost of the experiments. From this study, the performance of each ANN used in this research was measured with the mean square error percentage and it was observed that FFNN achieved the best results. Also the Pearson correlation coefficient was calculated to analyze the correlation between the five inputs (cutting speed, feed per tooth, axial depth of cut, chip's width, and chip's thickness) selected for the network with the selected output (surface roughness). Results showed a strong correlation between the chip thickness and the surface roughness followed by the cutting speed.

Keywords face milling, feed forward, generalized regression, radial base, surface roughness

1. Introduction

Surface roughness (arithmetic average, R_a) is commonly used as one of the principal methods to assess high-quality products in the manufacturing industries.

The ability of a workpiece to distribute and hold a lubricant as well as to accept a coating, resist fatigue, friction, and wear is related to its surface roughness. Also the interactions between the workpiece material-cutting tool-machining system have an impact on surface roughness, surface texture, and dimensional deviations of the product being machined.

The idea of predicting the surface roughness prior to machining has attracted a lot of attention, being the main goal of a number of research efforts.

An artificial neural network (ANN) is a mathematical model of a physical process which comprises a large number of processing elements organized into layers.

Before a network can perform a useful task, it has to be trained using a set of inputs and known outputs. Once trained, the network is able to give a particular answer for a given set of inputs.

In this article, several ANNs are developed to predict surface roughness on Al 7075-T7351 after face milling process. Five inputs (cutting speed, feed per tooth, axial depth of cut, chip's width, and chip's thickness) were considered for the development of the networks (Radial Base, Feed Forward and General Regression). The networks were compared between each other, selecting the one that achieved the best performance when comparing the predicted and measured surface roughness value.

Patricia Muñoz-Escalona, Departamento de Mecánica, Universidad Simón Bolívar, Caracas, Venezuela; and **Paul G. Maropoulos**, Department of Mechanical Engineering, University of Bath, Bath, UK. Contact e-mail: pmunoz@usb.ve.

2. Literature Review

Engineered components must satisfy surface texture requirements and, traditionally, surface roughness (arithmetic average, R_a) has been used as one of the principal methods to assess quality. The surface roughness value is a result of the cutting parameters and tool wear. Moreover, surface finish influences mechanical properties such as fatigue behavior, wear, corrosion, lubrication, and electrical conductivity. Thus, measuring and characterizing surface finish can be considered for predicting machining performance.

Luong and Spedding (Ref 1) applied neural network technology for the prediction of machining performance in metal cutting. Their network was trained using data from a machining data handbook. They concluded that the network was able to determine conditions for a given material and required depth of cut, and to predict the performance of the process in terms of cutting forces, surface finish, and tool life. Also they recognized that there is a lack of guidance on network design.

For the prediction of surface roughness, Benardos and Vosniakos (Ref 2) used a feed forward ANN. The experimental data was obtained after face milling Al alloy normally used in aerospace applications. They concluded that an ANN can be used reliably, successfully, and very accurately for the modeling of surface roughness formation mechanism and the prediction of its value in face milling.

In 2005, Bisht et al. (Ref 3) developed a back propagation neural network for the prediction of flank wear in turning operations. In their case, they included the chip width in

addition to the existing inputs (cutting speed, feed rate, depth of cut, and cutting forces). They concluded that the back propagation neural network could be trained for the effective prediction of flank wear during turning operations.

Pal and Chakraborty (Ref 4) predicted the surface roughness in a turning process by using a back propagation neural network. A large number of experiments were performed on mild steel using a high-speed cutting tool. They showed the efficacy of a back propagation neural network for predicting surface roughness in turning.

In 2006, Basak et al. (Ref 5) developed radial basis neural network models when turning AISI D2 cold-worked tool steel with ceramic tool. They identified the best values of cutting parameters for a desired value of surface roughness.

In 2006, Zhong et al. (Ref 6) predicted surface roughness heights R_a and R_t of turned surfaces using a neural network. The experiments were conducted using aluminum and copper rods of 19 mm diameter. Their study showed the effect of the neural network and hyperbolic tangent and sigmoid activation functions on the accuracy of the network.

The determination of best cutting parameters leading to a minimum surface roughness in end milling mold surfaces used in biomedical applications was done by Oktem et al. (Ref 7). For their research, they coupled a neural network and a genetic algorithm (GA) providing good results to solve the optimization of the problem.

In 2007, Lin et al. (Ref 8) developed a surface prediction model for high-speed machining 304L stainless steel, Al 6061-T6, SKD11, and Ti-4Al-4V. For this purpose, the finite element method and neural network were coupled, and they concluded that surface roughness may quickly be determined from the prediction model developed when the process parameters are set.

In 2007, Jesuthanam et al. (Ref 9) proposed the development of a novel hybrid neural network trained with GA and particle swarm optimization for the prediction of surface roughness. The experiments were carried out for end milling operations, and they found that the proposed hybrid neural network is competent in terms of computational speed and efficiency over the neural network model.

As it is observed once completing the literature review, most of the ANN has been developed for turning process giving less attention to face milling operations. Due to this fact and considering the importance of the face milling process in many industries, for example, the mold and die industry, the radial base (RBNN), feed forward (FFNN), and generalized regression (GRNN) neural networks architecture are developed in this research to help engineers in the manufacturing field to predict the desire surface roughness for a specific environment by selecting the optimum combination of cutting parameters.

3. Experimental Procedure

3.1 Workpiece Characteristics

Aluminum alloy 7075-T7351 square bars, $333 \times 76.2 \times 31.75$ mm^3 as suggested by ISO Standard 8688-1 (Ref 10), were used for the experiments. This material was selected for the experiments because it is widely used where low weight is needed such as in plates, sheet, and extrusions of airframes. Also, this Al alloy has some advantages such as good resistance, high strength, heat treatable, and high toughness. Table 1 and 2 show the chemical composition and the mechanical properties of the Al 7075-T7351 alloy, respectively.

3.2 Tool and Tip Characteristics

A standard insert holder of $Ø_{Tool} = 32$ mm with two cutting edges (inserts) $Z = 2$ were used for the experiments. As tool insert, SDHT 120508FR-ALP CWK26 (tool nose radius of 0.8 mm), was used as recommended by the tool suppliers for Al alloy under a wet cutting operation.

The $Ø_{Tool} = 32$ mm was selected to machine the whole width of the workpiece in a single pass since the tools diameter is bigger than the workpiece's width ($Ø_{Tool} = 32 > 31.75$ mm).

This condition ($Ø_{Tool} > W$) as well as a symmetric position between the tool and the workpiece will achieve a better performance of the tool (longer tool life) as suggested by Diniz and Filho (Ref 11). Figure 1 shows a scheme of the cutting process.

3.3 Cutting Parameters

Cutting speed, feed per tooth, and the axial depth of cut were the variables chosen for the study because from previous research it was observed that these variables had the most influence on surface roughness and tools life. A low, medium, and high level was selected for each of the cutting parameter to have a wide range of combinations. Also the selected values are recommended from the tool supplier when cutting Al alloy under wet cutting conditions.

Selected cutting parameters are shown in Table 3.

Table 1 Chemical composition of Al 7075-T7351

%Al ± 0.1	%Cr ± 0.01	%Cu ± 0.01	%Mg ± 0.01	%Zn ± 0.01
87.1-91.4	0.18-0.28	1.20-2.00	2.10-2.90	5.10-6.10

Table 2 Mechanical Properties of Al 7075-T7351

Ultimate strength, MPa	593
Yield strength, MPa	448
Brinell hardness(a)	135

(a) Load = 500 kg and $Ø_{ball} = 10$ mm

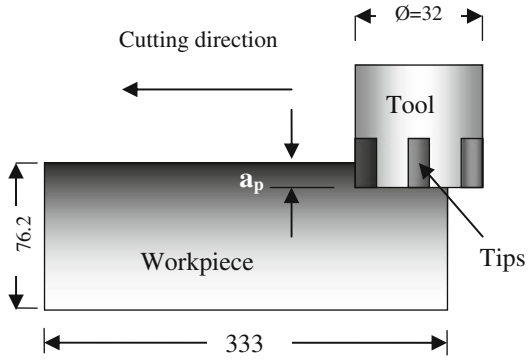

Fig. 1 Scheme of the cutting process

3.4 Equipment Characteristics

A Deckel Maho, DMV 50 eVolution, high-speed vertical machine center with a maximum spindle speed of 18,000 rpm was used for the face milling operations.

The tests were conducted under MQL (minimum quantity of lubricant) since tool wear was not considered as a criterion that will affect the result of the cutting process due to the fact that Al 7075-T7351 is a very soft material and the cutting process was conducted under wet cutting conditions.

3.5 Design of Experiments: Taguchi Method

An efficient method of experimental planning is design of experiments (DoE), which incorporates the orthogonal arrays (OAs), developed by Taguchi, to successfully design and conduct fractional factorial experiments that can collect all the statistically significant data with the minimum possible number of repetition.

The selection of the appropriate OA is based on the following criteria: the numbers of factors and interactions of interest, the numbers of levels for the factors of interest, and the desired experimental resolution or cost limitation (Ref 12).

Although a three-level factor is considered as a small OA, due to cost and time saving the L9 array was selected, and Table 4 shows the OA for the three cutting parameters selected. The values 1 to 3 indicate the levels of the three cutting parameters as these are defined in Table 3.

3.6 Roughness Measurements

A Profilometer, ProScan 2000, using a white lamp was used for the measurement of R_a values. The sample size used for this case was 4 mm in the X direction and 4 mm in the Y direction, and 1335 steps with a size of 0.003 mm each to cover this 4×4 mm^2 area was used in the experiments as recommended in the ProScan manufacturer's guide for face milling operations.

Three measurements were taken in each sample after cutting a length of 333 mm as shown in Fig. 2.

Table 3 Selected cutting parameters

Level	*V*, m/min	fz, mm/rev × tooth	ap, mm
Low (1)	600	0.1	3.0
Medium (2)	800	0.2	3.5
High (3)	1000	0.3	4.0

V, cutting speed; fz, feed per tooth; and ap, axial depth of cut

Table 4 L_9 orthogonal array for the experiments

Trial	*V*, m/min	fz, mm/rev × tooth	ap, mm
1	1	1	1
2	1	2	2
3	1	3	3
4	2	1	2
5	2	2	3
6	2	3	1
7	3	1	3
8	3	2	1
9	3	3	2

Because there was no difference between each of the three surface roughness measurements made in each sample, an average of them was taken and considered as the roughness of the specimen for a specific cutting condition.

3.7 Chip Measurement

Due to the importance of the chips geometry on the surface roughness, since it's related to the feed and axial depth of cut, the chips generated from each trial were collected and measured to include these variables as one of the inputs of the networks.

The chip's width (C_w) was measured with an Olympus SZ61 optical magnifier at ×12, and for the chip's thickness (C_t) measurement, a TESSA micrometer with a range of 0 to 25 mm with a resolution of 0.01 mm was used. Each dimension (width and thickness) was measured three times, reporting only the average values for each of them.

3.8 The Artificial Neural Network

An ANN consists of a number of elementary units called neurons. A neuron is a simple processor which takes one or more inputs and produces an output. Each input has an associated weight that determines the intensity of the input. A network can be trained to perform certain tasks where the data is fed into the network through an input layer. This is processed through one or more intermediate hidden layers and finally it is fed out to the network through an output layer as shown in Fig. 3.

The MATLAB 6.5 software, Neural Network Toolbox function, was used to create, train, validate, and predict the different ANN reported in this research.

It must be highlighted that the best network architecture is reached by trial and error after considering different

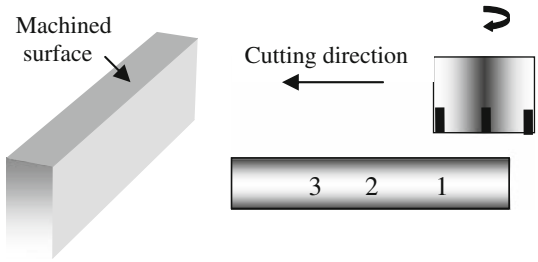

Fig. 2 Scheme indicating the areas where surface roughness measurements were taken

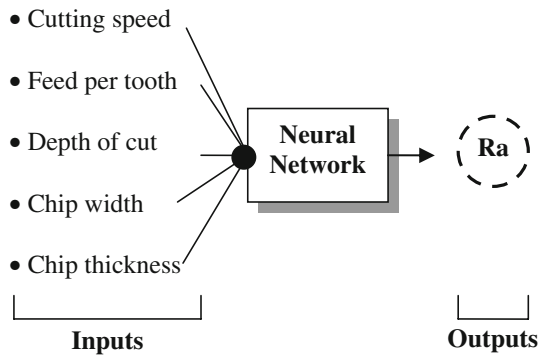

Fig. 3 Inputs and outputs of the network

combinations of the number of neurons in the hidden layer, number of hidden layers, spread parameter, and learning rate, depending on the type of neural network being used.

From the nine trials, six of them were picked randomly (1, 3, 5, 6, 7, and 8) and were used for training and validating the network, and the other three trials (2, 4, and 9) were used for predicting.

During the training of the network, the calculated output is compared to the target output, and then the mean square error percentage (%MSE) is calculated by using Eq 1.

$$\%\mathrm{MSE}_X = \left|\frac{R_a - R_{aX}}{R_a}\right| \cdot 100, \qquad \text{(Eq 1)}$$

where $\%\mathrm{MSE}_X$ is the Mean Square Error in %, R_a is the measured surface roughness (μm). X is either trained or predicted depending on the case.

3.8.1 Radial Base Neural Network. This network architecture can be designed in a very short period of time since it consists of three layers: (1) input layer, (2) hidden layer, and (3) output linear layer.

There are only two types of radial base networks, the *newrbe* (exact design) and the *newrb* (more efficient design). For this study, the *newrb* was selected since this architecture interactively creates one neuron at a time. Neurons are added to the network until the sum-squared error falls beneath an error goal or a maximum numbers of neurons have been reached (MATLAB user's guide, Ref 13).

3.8.2 Feed Forward Neural Network. This network is one of the most popular multi-layer architectures proving to be an excellent universal approximation of nonlinear functions. Its ability to map complex input-to-output relationships with acceptable error best demonstrates its suitability. There are many variations of feed forward networks and in this case, the Lavenberg-Marquardt algorithm was selected. This algorithm is designed to approach second-order training speed without having to compute the Hessian Matrix, being the fastest method for training moderate-sized FFNNs.

3.8.3 Generalized Regression Neural Network. This type of network is often used for function approximation. It has a radial basis layer and a special linear layer. The first layer is just like the *newrbe* network and it has as many neurons as there are input/target vectors.

3.9 Experimental Setup

Figure 4 shows a scheme of the experiment setup used in this research. As it is observed once each trial was concluded, experimental surface roughness was measured and chip was collected for further measurement. The ANNs were developed considering cutting parameters and chips geometry as input variables and the surface roughness as the output variable. The predicted surface roughness obtained from each developed ANN was compared with experimental (measured) values of surface roughness.

Figure 5 shows the flow chart used for the three networks studied in this research to reach the minimum %MSE for trained and predicted values of surface roughness.

3.10 Pearson Correlation Coefficient

To clarify the matching between surface roughness and the inputs studied (cutting speed, feed per tooth, axial depth of cut, chip's width, and chip's thickness), a correlation among these parameters is determined.

A correlation is a statistical technique which can show whether and how strongly pairs of variables are related. The main result of a correlation is called correlation coefficient (or r). It ranges from −1.0 to +1.0. The closer the r is to +1 or −1, the more closely the two variables are related.

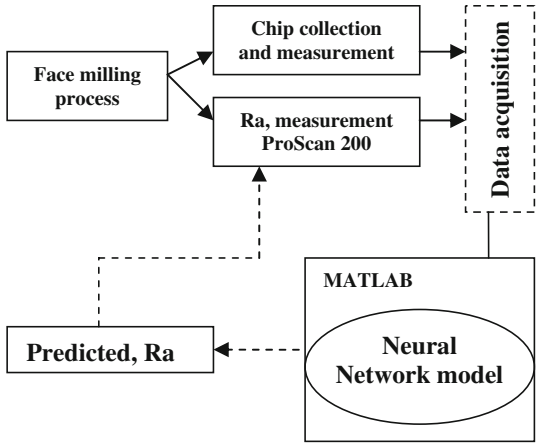

Fig. 4 Diagram of the experimental setup

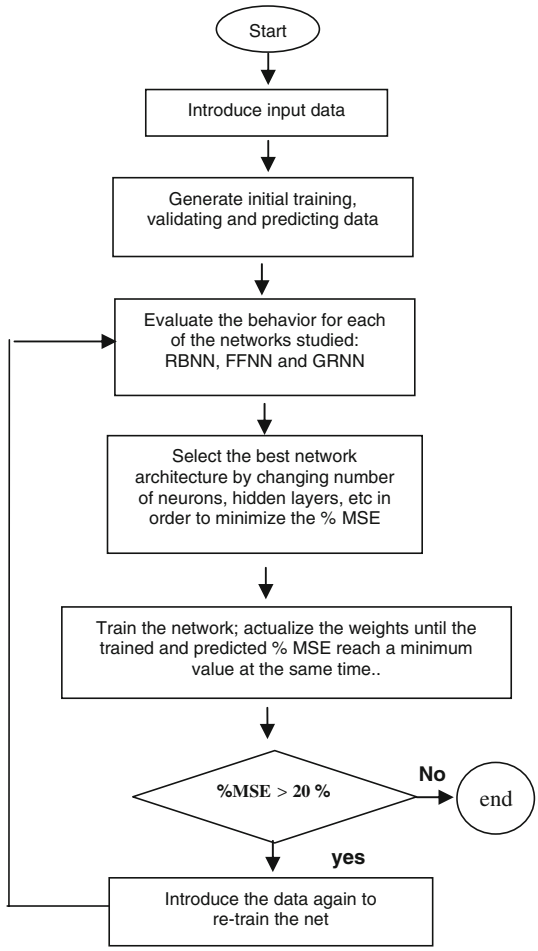

Fig. 5 Flow chart to reach a minimum %MSE at the same time for trained and predicted values of surface roughness

If r is close to 0, it means that there is no relationship between the variables. If r is positive, it means that as one variable gets larger, the other gets larger. If r is negative, it means that as one gets larger, the other gets smaller (often called an inverse correlation). There are several different correlation techniques but the most common one is the Pearson correlation and this is the one that has been selected for this study.

4. Results and Discussions

Once all the experiments were concluded, the following results were obtained and divided in five subsections for better understanding.

4.1 Values of Surface Roughness (R_a) Measured with the ProScan 2000 Profilometer

Table 5 shows the surface roughness average values obtained once the face milling process was concluded for specific cutting conditions.

4.2 Chip Measurement

Table 6 shows the average value of the chip's width and thickness once the face milling process was concluded for a specific cutting condition.

As reported in section 3.7, chip's area (width and thickness) depends on the axial depth of cut and the feed per tooth. As it can be observed, chip's width values obtained and reported in Table 6 are almost the same as the axial depth of cut values selected for the experiments, but there are some differences in the values of the chip's thickness reported in Table 6 when compared to the feed per tooth values used in this work. This result is probably due to the fact that since new tips are screwed into the tool holder for each trial, generating a discrepancy in the location of the cutting tools teeth and the cutter axis inclination with regards to the direction that must be maintained during the cutting process. This is what Franco et al. (Ref 14) called tool errors or radial and axial runouts.

Table 5 Surface roughness and average surface roughness obtained from face milling operations under different cutting conditions

Trial	V, m/min	fz, mm/rev × tooth	ap, mm	R_a 1, µm	R_a 2, µm	R_a 3, µm	R_a aver(a), µm
1	600	0.1	3.0	0.645	0.650	0.713	0.699
2	600	0.2	3.5	1.075	1.078	0.899	1.017
3	600	0.3	4.0	1.566	1.472	1.662	1.566
4	800	0.1	3.5	0.626	0.586	0.679	0.630
5	800	0.2	4.0	0.8	0.85	0.864	0.838
6	800	0.3	3.0	0.6	0.657	0.682	0.646
7	1000	0.1	4.0	0.712	0.702	0.723	0.712
8	1000	0.2	3.0	0.892	0.831	0.872	0.865
9	1000	0.3	3.5	0.72	0.697	0.717	0.711

(a) R_a, average of measured surface roughness which will be considered as the surface roughness of the specimen for a specific cutting condition

4.3 Artificial Neural Network

4.3.1 Radial Base Neural Network. To start the training of this neural network, five inputs (cutting speed, feed per tooth, axial depth of cut, chip's width, and chip's thickness), six neurons in the hidden layer, a goal of 0.01, and a spread parameter of 0.8 varying it every 0.05 were considered.

In Fig. 6, goal's performance for this radial base network is observed. Also, this figure shows how a goal of 0.01 is reached around 2.6 epochs.

Since the goal value of 0.01 was reached so soon (before reaching 3 epochs), then three neurons instead of six were considered in the hidden layer.

Figure 7 shows the architecture of the RBNN selected and used in this study, where number 5 represents the number of inputs, number 3 the number of neurons in the hidden layer, and number 1 the number of outputs, in our case the surface roughness value.

Table 7 shows the surface roughness ($R_{a\mathrm{T}}$) obtained by training the network for a goal of 0.01 and different spread parameter. Also, measured surface roughness (R_a) is shown.

Due to the small amount of values for training the network, it is observed that a spread parameter from 0.05 to 0.3 gave smaller %MSE, but as it was consulted in the literature (MATLAB user's guide), the spread parameter must be large

Table 6 Chip's width (C_w) and thickness (C_t) obtained from face milling operations under different cutting conditions

Trial	V, m/min	fz, mm/rev × tooth	ap, mm	C_w, mm	C_t, mm
1	600	0.1	3.0	3.0	0.20
2	600	0.2	3.5	3.5	0.20
3	600	0.3	4.0	4.0	0.45
4	800	0.1	3.5	3.5	0.22
5	800	0.2	4.0	4.0	0.17
6	800	0.3	3.0	3.0	0.22
7	1000	0.1	4.0	3.8	0.18
8	1000	0.2	3.0	3.0	0.3
9	1000	0.3	3.5	3.5	0.35

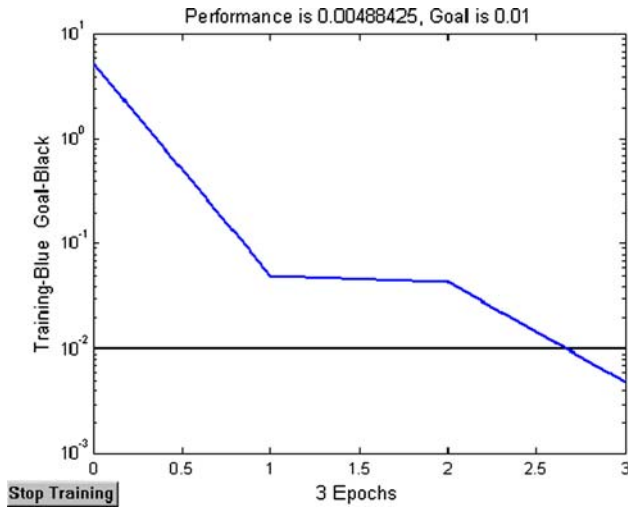

Fig. 6 Goal performance for radial base network

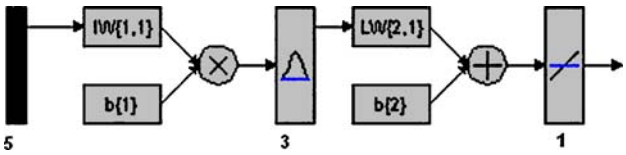

Fig. 7 Radial base network architecture used in this study

Table 7 Spread parameter, measured and trained surface roughness (R_a, R_{aT}), and %MSE obtained by training the RBNN with a goal of 0.01 and 3 neurons in the hidden layer

R_a, μm	1 0.699	3 1.566	5 0.838	6 0.646	7 0.712	8 0.865	
R_{aT}, μm	1	3	5	6	7	8	%MSE
Spread							
0.05	0.686	1.566	0.838	0.686	0.686	0.865	7.42
0.1	0.686	1.566	0.838	0.686	0.686	0.865	7.42
0.15	0.686	1.566	0.838	0.686	0.686	0.865	7.42
0.2	0.686	1.566	0.838	0.686	0.686	0.865	7.42
0.25	0.686	1.566	0.838	0.686	0.686	0.865	7.42
0.3	0.686	1.566	0.838	0.686	0.686	0.865	7.43
0.35	0.686	1.566	0.838	0.686	0.686	0.865	7.48
0.4	0.685	1.566	0.837	0.687	0.685	0.865	7.64
0.45	0.685	1.566	0.837	0.689	0.685	0.865	7.93
0.5	0.685	1.566	0.835	0.691	0.684	0.865	8.31
0.55	0.685	1.566	0.833	0.693	0.682	0.866	8.68
0.6	0.688	1.566	0.831	0.695	0.680	0.866	8.97
0.65	0.692	1.566	0.829	0.695	0.677	0.867	9.16
0.7	0.699	1.566	0.827	0.694	0.672	0.869	9.34
0.75	0.707	1.565	0.825	0.691	0.667	0.871	9.61
0.8	0.716	1.564	0.824	0.687	0.661	0.873	10.11

Table 8 Measured and predicted surface roughness and mean square error when training the RBNN with a goal of 0.01 and a spread of 0.6

Trial	R_a, μm	R_{aP}, μm	%MSE
2	1.017	0.969	
4	0.630	0.731	17.32
8	0.711	0.741	

enough that the radial base neurons respond to overlapping regions of the input space, but not so large that all the neurons will respond in essentially the same manner. For this reason, the network was trained again, but in this case, the network was stopped when the calculated surface roughness values obtained when training the network (R_{aT}) and the predicted surface roughness values (R_{aP}) showed at the same time the minimum %MSE when comparing them to the target output which is the measured surface roughness (R_a). In our case, this value was reached when using a spread parameter of 0.6.

Table 8 shows the measured and predicted surface roughness value (R_a and R_{aP}) obtained when using three neurons in the hidden layer, a goal of 0.01, and a spread parameter of 0.6.

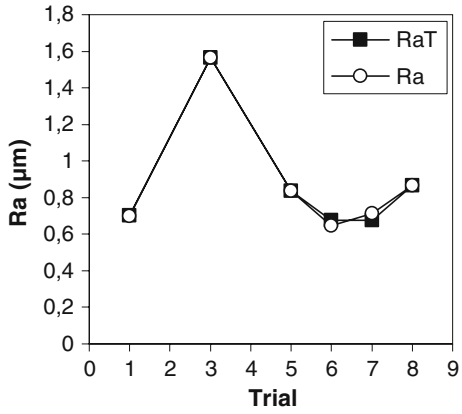

Fig. 8 Measured and trained values of surface roughness for different trials using the selected RBNN architecture

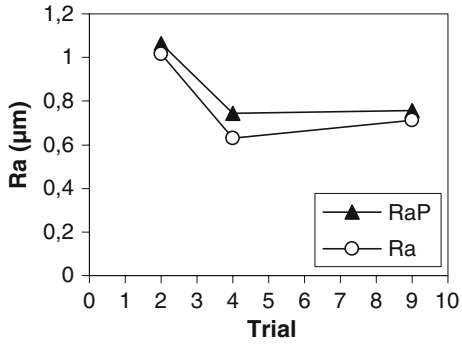

Fig. 9 Measured and predicted values of surface roughness for different trials using the selected RBNN architecture

As it can be observed in Table 8, a %MSE of 17.32 between the measured (R_a) and the predicted values of surface roughness (R_{aP}) was obtained by using the selected RBNN.

Figure 8 shows the results obtained with the measured and trained surface roughness, and Fig. 9 shows the results of the measured and predicted values of surface roughness.

4.3.2 Feed Forward Network. For this neural network, same as the RBNN, five inputs (cutting speed, feed per tooth, depth of cut, chip width, and chip thickness) were considered.

The Lavenberg-Marquardt algorithm was selected and from trial and error, a maximum of two hidden layers and a maximum of nine neurons were used. The activation function for the three layers architecture network (input layer, hidden layer, and output layer) were *tansig* and *purelin*, and the activation function for the four layers architecture network (input layer, hidden layer 1, hidden layer 2, and output layer) were *tansig*, *logsig*, and *purelin*. Also, a goal of 0.01, 100 epochs, and a maximum of 400 iterations were used. This number of iterations corresponds to the minimum %MSE obtained by the trained and predicted values of surface roughness at the same time.

Table 9 shows just few numbers of the total iterations, the FFNN architecture, the trained surface roughness (R_{aT}), and the trained and predicted mean square error, $\%MSE_T$ and $\%MSE_P$, respectively.

As it is observed in Table 9, the FFNN architecture that achieved the minimum %MSE for both trained and predicted

Table 9 FFNN architecture, trained surface roughness (R_{aT}), MSE_T, and MSE_P

No. of hidden layer	No. of iterations	Network architecture	R_a1_T	R_a3_T	R_a5_T	R_a6_T	R_a7_T	R_a8_T	$\%MSE_T$	$\%MSE_P$
1	43	5-2-1	0.686	1.518	0.856	0.630	0.712	0.711	18.4	14.6
1	2	5-3-1	0.744	1.453	0.812	0.680	0.675	0.720	21.0	15.4
2	278	5-2-4-1	0.652	1.434	0.861	0.672	0.702	0.756	17.4	12.9
2	23	5-2-5-1	0.711	1.518	0.852	0.620	0.704	0.713	18.5	13.7
2	6	5-2-6-1	0.690	1.418	0.860	0.631	0.706	0.870	10.2	9.5
2	61	5-2-7-1	0.694	1.539	0.833	0.687	0.749	0.974	15.2	13.5
2	222	5-3-6-1	0.683	1.564	0.819	0.697	0.683	0.752	16.1	9.6
2	107	5-3-7-1	0.701	1.434	0.838	0.647	0.703	0.861	8.5	5.5
2	4	5-7-2-1	0.712	1.548	0.812	0.776	0.728	0.894	20.8	16.3
2	81	5-7-3-1	0.812	1.551	0.773	0.625	0.718	0.778	20.8	21.6
2	200	5-7-4-1	0.721	1.520	0.839	0.677	0.678	0.762	14.4	16.2
2	92	5-7-5-1	0.662	1.572	0.746	0.675	0.616	0.825	19.2	21.4
2	108	5-7-6-1	0.727	1.527	0.796	0.572	0.727	0.715	21.9	16.3
2	86	5-7-7-1	0.733	1.523	0.883	0.733	0.734	0.733	22.0	18.2
2	15	5-8-3-1	0.704	1.323	0.864	0.649	0.712	0.861	15.8	11.5
2	93	5-9-8-1	0.718	1.461	0.899	0.746	0.735	0.742	23.6	18.4

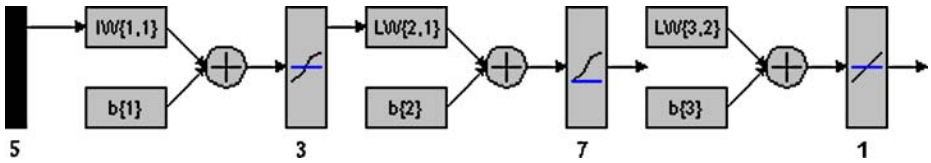

Fig. 10 Feed forward architecture network selected for the study

Table 10 Measured (R_a) and predicted (R_{aP}) surface roughness and %MSE when using a feed forward architecture network 5-3-7-1

Trial	R_a, μm	R_{aP}, μm	$\%MSE_P$
2	1.017	1.0188	
4	0.63	0.6457	5.5
9	0.711	0.74569	

surface roughness value is 5-3-7-1. Also it observed an error of 8.5% between the measured roughness (R_a) and the trained surface roughness (R_{aT}), and an error of 5.5% between the measured roughness (R_a) and the predicted surface roughness (R_{aP}), was obtained.

Figure 10 shows the architecture of the selected feed forward network.

Table 10 shows the measured and predicted surface roughness values (R_a and R_{aP}, respectively) obtained when using this 5-3-7-1 FFNN architecture on trials 2, 4, and 9.

Figure 11 shows the results obtained with the measured and trained surface roughness, and Fig. 12 shows the results of the measured and predicted values of surface roughness for the 5-3-7-1 FFNN architecture.

4.3.3 Generalized Regression Neural Network. To start the training of this GRNN, a spread parameter of 0.8 varying it every 0.05 was selected, and from this result, it was observed that the minimum % MSE was obtained with a spread parameter of 0.3.

Due to this fact, an extra training was done with a spread parameter of 0.3 but varying this last one every 0.005. Also, the algorithm was built to show the minimum %MSE between the measured and the trained and predicted value of surface roughness at the same time.

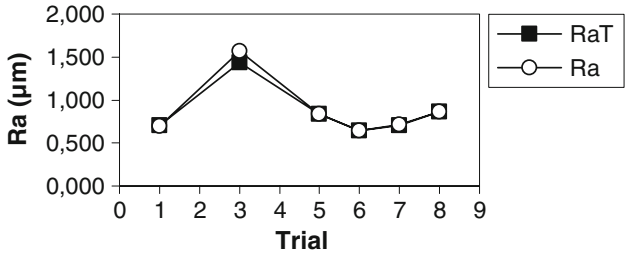

Fig. 11 Measured and trained surface roughness for a 5-3-7-1 feed forward architecture network

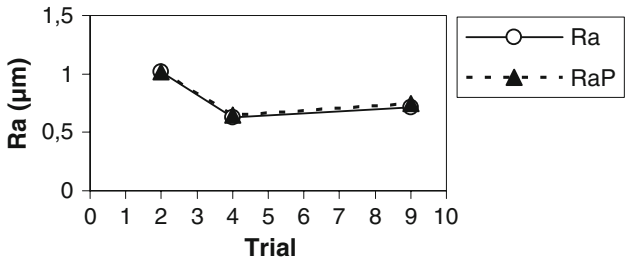

Fig. 12 Measured and predicted surface roughness for a 5-3-7-1 feed forward architecture network

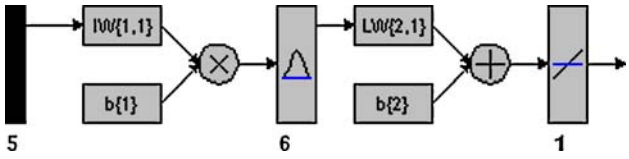

Fig. 13 Generalized regression architecture network selected for the study

Table 11 Measured (R_a) and predicted (R_{aP}) surface roughness, $\%MSE_T$, and $\%MSE_P$ when using a GRNN with a spread of 0.295

Trial	R_a, µm	R_{aP}, µm	$\%MSE_T$	$\%MSE_P$
2	1.017	1.0268		
4	0.630	0.7525	0.011	20.90
9	0.711	0.7650		

Table 12 Minimum %MSE predicted obtained for the different selected ANN architecture

Network	Architecture	$\%MSE_T$	$\%MSE_P$
RBNN	5-3-1	8.97	17.32
FFNN	5-3-7-1	8.5	5.5
GRNN	5-6-1	0.012	20.90

The selected GRNN architecture showed a minimum %MSE with a spread parameter of 0.295.

Figure 13 shows the architecture of the GRNN, with five inputs, six neurons in the hidden layer, and 1 output.

Table 11 shows the result of measured, trained, and predicted surface roughness as well as the minimum %MSE obtained with the selected GRNN architecture.

4.4 Performance Assessment

The performance of each ANN used in this research was measured with the mean square error (%MSE).

Table 12 shows the minimum %MSE obtained for each selected architecture, and Fig. 14 and 15 illustrates this performance for trained and predicted values of surface roughness, respectively.

When comparing the %MSE of the three selected studied architecture shown in Table 12, it is observed that the FFNN shows the closest and minimum result when training the network and when predicting the values of roughness. In this case, a 5.5% of difference between the predicted and the measured values of surface roughness can be interpreted as a very good approach.

Also, it is observed that a low $\%MSE_T = 0.012$ is obtained when training the GRNN and this is due to the fact that this type of net uses a maximum number of neurons equal to the maximum numbers of trials used to train the net; with this fact and an adequate spread parameter, the difference between the measured and the trained roughness is null since an exact RBNN (*newrb*) was used.

4.5 Pearson Correlation Coefficient Analysis

Table 13 shows the Pearson correlation coefficient obtained for each parameter.

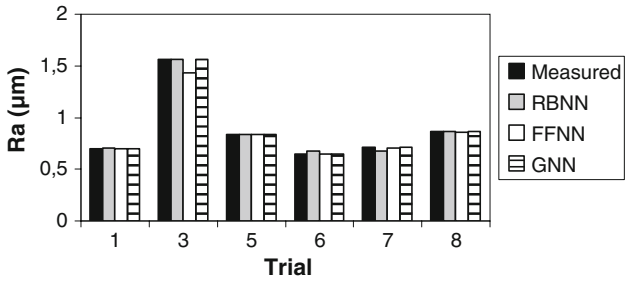

Fig. 14 Comparison of trained and measured surface roughness obtained for each selected network for different trials

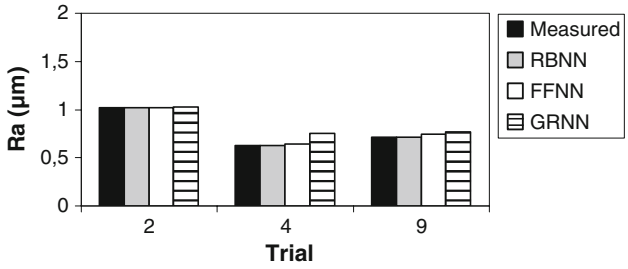

Fig. 15 Comparison of predicted surface roughness obtained for each selected network for different trials

Table 13 Pearson correlation coefficient among surface roughness and inputs studied

	V	fz	ap	C_w	C_t	R_a
V	1.00	0.00	0.00	−0.07	0.10	−0.49
fz	0.00	1.00	0.00	0.07	0.68	0.43
ap	0.00	0.00	1.00	0.99	0.10	0.44
C_w	−0.07	0.07	0.99	1.00	0.16	0.50
C_t	0.10	0.68	0.10	0.16	1.00	0.53
R_a	−0.49	0.43	0.44	0.50	0.53	1.00

From Table 13 it can be observed that there is a strong correlation between the chip thickness (C_t) and the chip width (C_w) on the surface roughness since a correlation coefficient value of 0.53 and 0.50 was obtained, respectively. From the cutting parameters, the strongest correlation is between the cutting speed and the surface roughness (−0.49), but in this case, it is a negative correlation, which means that the magnitude of surface roughness is increased as the cutting speed is decreased. This result is in agreement with previous researches (Ref 15, 16).

5. Conclusions

In this study, ANNs with five inputs have been developed to predict arithmetic surface roughness (R_a) when face milling Al 7075-T7351.

FFNN showed the best results ($\%MSE_P = 5.5$) but it took more time training this network compared to the RBNN and the GRNN.

Due to the fact that the outcome of the training greatly depends on the initialization of the weights, which is done randomly by the MATLAB software, each ANN must be trained few times until the minimum %MSE between the trained and predicted surface roughness against the measured surface roughness is achieved.

From Pearson correlation analysis, the cutting speed is the most important cutting parameter affecting the machined surface quality.

References

1. L.H.S. Luong and T.A. Spedding, A Neural Network System for Predicting Machining Behavior, *J. Mater. Process. Technol.*, 1995, **52**, p 585–591
2. P.G. Benardos and G.C. Vosniakos, Prediction of Surface Roughness in CNC Face Milling Using Neural Networks and Taguchi's Design of Experiments, *Robot. Comput. Integr. Manuf.*, 2002, **18**, p 343–354
3. H. Bisht, J. Gupta, S.K. Pal, and D. Chakraborty, Artificial Neural Network Based Prediction of Flank Wear in Turning, *Int. J. Mater. Prod. Technol.*, 2005, **22**(4), p 328–338
4. S. Pal and D. Chakraborty, Surface Roughness Prediction in Turning Using Artificial Neural Network, *Neural Comput. Appl.*, 2005, **14**, p 319–324
5. S. Basak, U.S. Dixit, and J.P. Davim, Application of Radial Basis Function Neural Networks in Optimization of Hard Turning of AISI D2 Cold-Worked Tool Steel with Ceramic Tool, *Proc. Inst. Mech. Eng. B: J. Eng. Manuf.*, 2007, **221**(6), p 987–998
6. Z.W. Zhong, L.P. Khoo, and S.T. Han, Prediction of Surface Roughness of Turned Surfaces Using Neural Networks, *Int. J. Adv. Manuf. Technol.*, 2006, **28**, p 688–693
7. H. Oktem, T. Erzurumlu, and F. Erzincanli, Prediction of Minimum Surface Roughness in End Milling Mold Parts Using Neural Network and Genetic Algorithm, *Mater. Des.*, 2006, **27**, p 735–744
8. S.Y. Lin, S.H. Cheng, and C.K. Chang, Construction of a Surface Roughness Prediction Model for High Speed Machining, *J. Mech. Sci. Technol.*, 2007, **21**, p 1622–1629
9. C.P. Jesuthanam, S. Kumanan, and P. Asokan, Surface Roughness Prediction Using Hybrid Neural Networks, *Mach. Sci. Technol.*, 2007, **11**, p 271–286
10. "Tool Life Testing in Milling. Part 1: Face Milling," ISO 8688-1, *International ISO Standard*, 1989
11. A. Diniz and J. Filho, Influence of the Relative Position of Tool and Workpiece on Tool Life, Tool Wear and Surface Finish in the Face Milling Process, *Wear*, 1999, **232**, p 67–75
12. D.C. Montgomery, *Design and Analyses of Experiments*, 3rd ed., John Wiley & Sons, New York, 1997
13. MATLAB User's Guide
14. P. Franco, M. Estrems, and F. Faura, Influence of Radial and Axial Runouts on Surface Roughness in Face Milling with Round Insert Cutting Tools, *Int. J. Machine Tools Manuf.*, 2004, **44**, p 1555–1565
15. D.A. Axente and R.C. Dewes, Surface Integrity of Hot Work Tool Steel after High Milling Experimental Data and Empirical Models, *J. Mater. Process. Technol.*, 2002, **127**, p 325–335
16. W. Bouzid and K. Sai, Roughness Modeling in Up-Face Milling, *Int. J. Adv. Manuf. Technol.*, 2005, **26**, p 324–329